

Diamond Detectors

Alexander Oh
University of Manchester

56

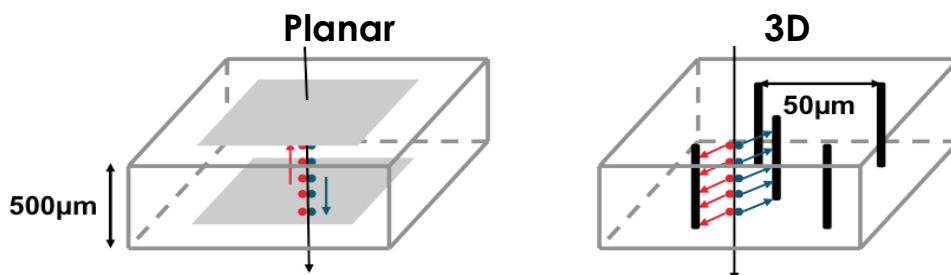
PART 2

- 3D Diamond detectors
- Application of diamond detectors in HEP

3D diamond detectors

28.05.24

3D Diamond Detectors

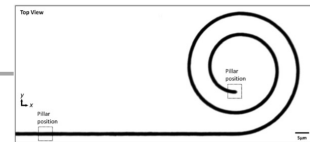
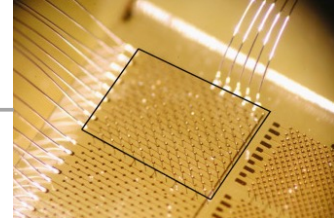
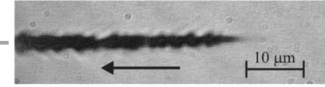


- Electrode spacing determines drift distance to induce 1e charge.
- 3D has shorter electrode spacing compared to planar.
- Charge carriers need less drift distance (and time) in 3D then in planar to induce equal signal.
- Influence of traps and resulting limited lifetime suppressed in 3D.

28.05.24

3D Diamond Research - A relatively young field

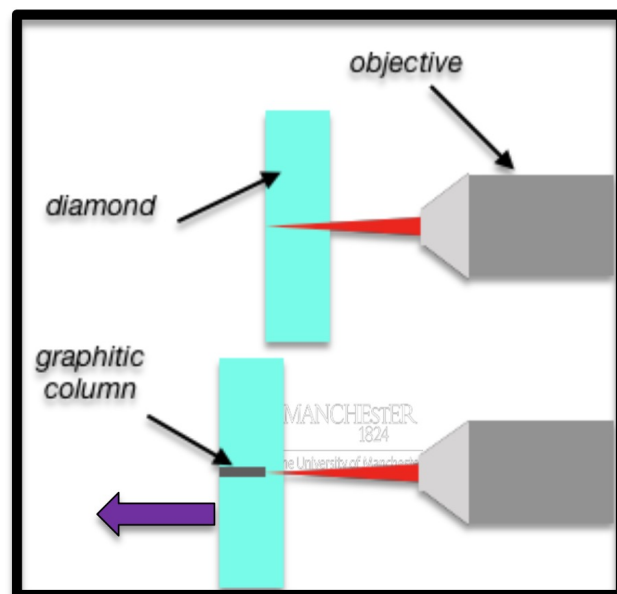
- Laser induced phase change in diamond.
 - E.g. T.V. Kononenko et al, Diamond & Related Materials 18 (2009) 196–199
"Femtosecond laser microstructuring in the bulk of diamond"
- 3D "Pad" detector
 - A. Oh, B. Caylar, M. Pomorski, T. Wengler, Diamond and Related Materials, 38, (2013), "A novel detector with graphitic electrodes in CVD diamond"
 - S. Lagomarsino et al, Appl. Phys. Lett. 103, 233507 (2013), "Three-dimensional diamond detectors: Charge collection efficiency of graphitic electrodes"
- 3D "strip array" detector with position resolution.
 - E.g. F. Bachmaier et al, NIM A, 786, (2015) 97-104,
"A 3D diamond detector for particle tracking"
- Radiation damage studies.
 - Eg. S. Lagomarsino et al, Applied Physics Letters 106, 193509 (2015)
"Radiation hardness of three-dimensional polycrystalline diamond detectors"
- Improvements in graphitization process.
 - Eg. B. Sun et al., Applied Physics Letters 105, 231105 (2014), "High conductivity micro-wires in diamond following arbitrary paths"
- 3D pixel detectors
 - RD42, CERN-LHCC-2018-015 ((2018), Development of Diamond Tracking Detectors for High Luminosity Experiments at the LHC, HL-LHC and Beyond
 - L. Anderlini et al, Front. Phys., 04 November 2020, Fabrication and Characterisation of 3D Diamond Pixel Detectors With Timing Capabilities



28.05.24

Fabrication

- Conductive columns are created by changing diamond into a graphitic material with a short laser pulse:



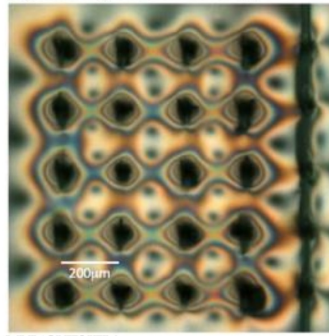
Laser graphitisation of diamond

28.05.24

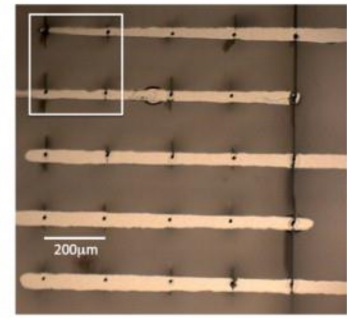
FIRST 3D DIAMOND DEVICE

- Collaboration of **Manchester**, CEA LIST and CERN
- Published **2013**
- Single crystal substrate
- First device made at LIST using **nano-second** pulse nitrogen laser with beam spot diameter of **10 μ m**

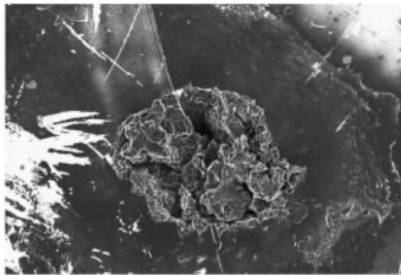
(a) Birefringence microscopy.



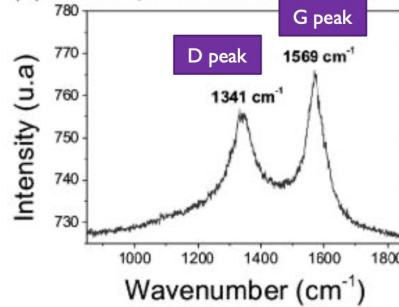
(b) Photograph after metallisation.



(a) SEM picture of a graphitic column.



(b) Raman spectrum on the graphitic column.



Oh, A., Caylar, B., Pomorski, M., & Wengler, T. (2013). A novel detector with graphitic electrodes in CVD diamond. *Diamond and Related Materials*, 38, 9–13.

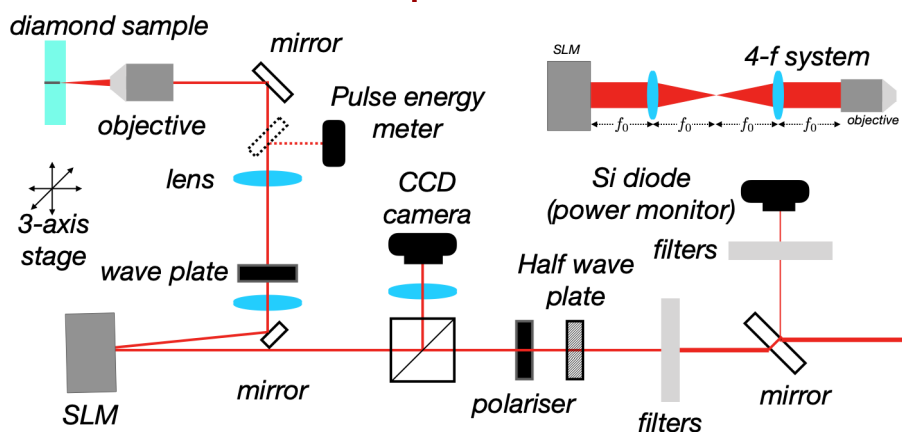
28.05.24

MANCHESTER
1824

Laser Set-up in Manchester

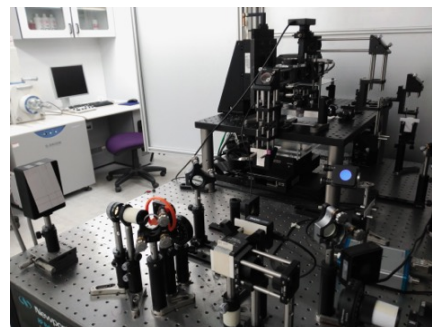
64

The University of Manchester



Laser specs:

- Wavelength: 800 nm
- Repetition rate: 1 kHz
- Pulse duration: 100 fs
- Max power: 1 W

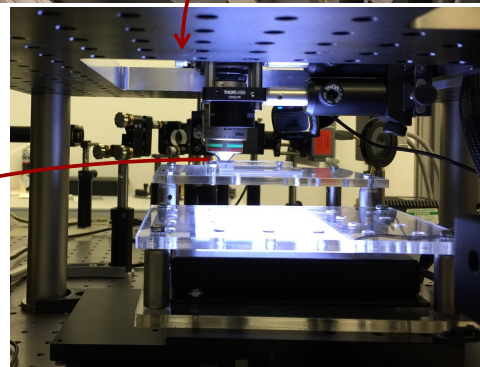
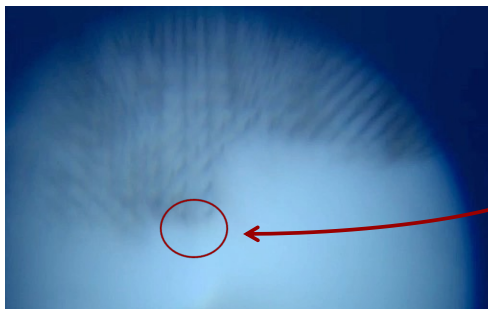
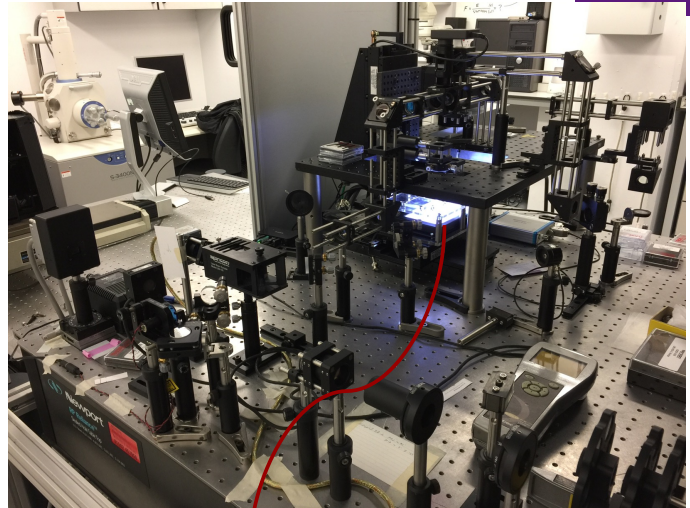


Just moved to MECDI

28.05.24

University of Manchester, Laser Processing Research Center.

- Wavelength = 800 nm
- Repetition rate = 1 kHz
- Pulse duration = 100 fs
- Spot size = 10µm
- Pulse Energy ~ 1 µJ
- **Spatial light modulator**

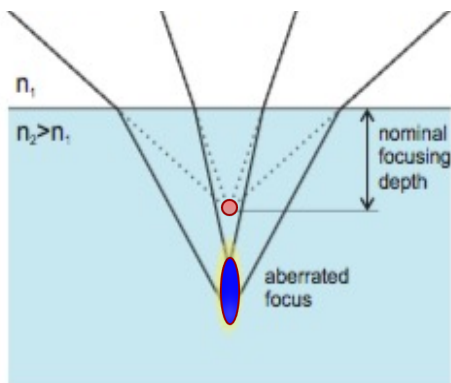


28.05.24

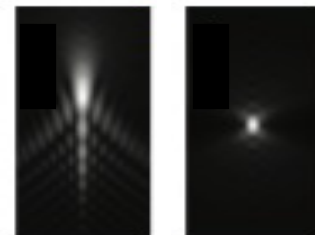
SLM – Phase Spatial Light Modulation

- Comparison SLM vs standard process.

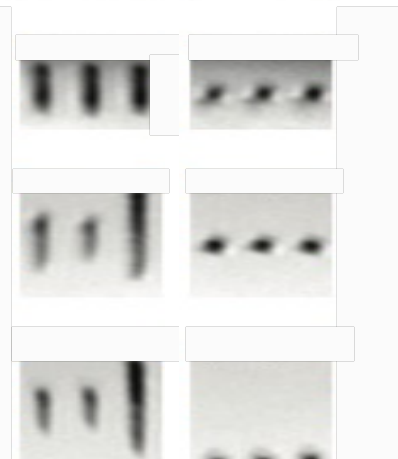
	Std.	SLM
Resistivity	1 Ωcm	0.1 Ωcm
Diameter	~3µm	~1µm
Diamond to graphite ratio	~4	~0.2



Simulated depth = 40µm



Measured depth = 40µm



depth = 80µm

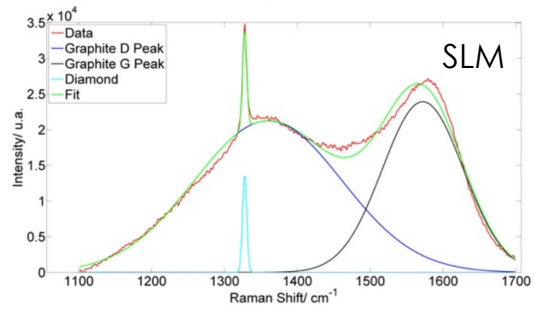
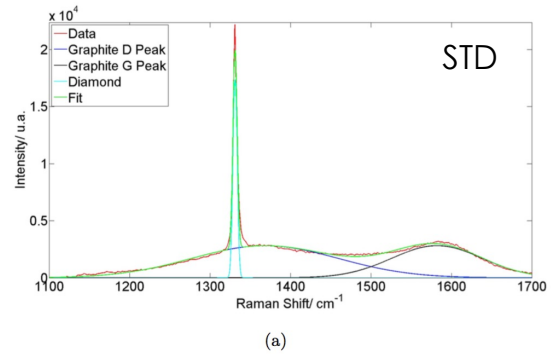
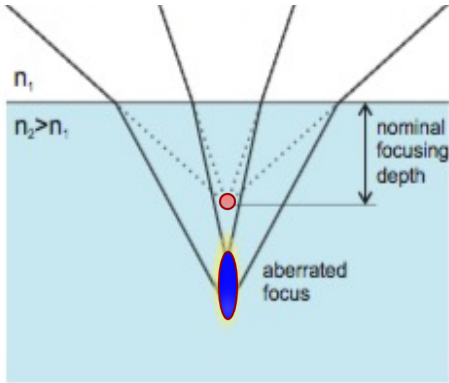
depth = 130µm

28.05.24

SLM – Phase Spatial Light Modulation

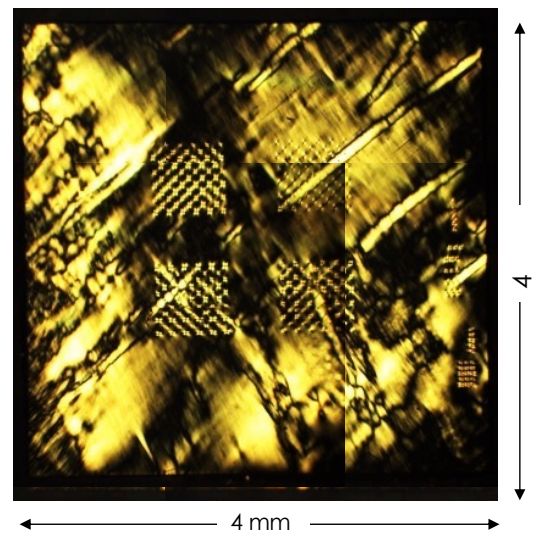
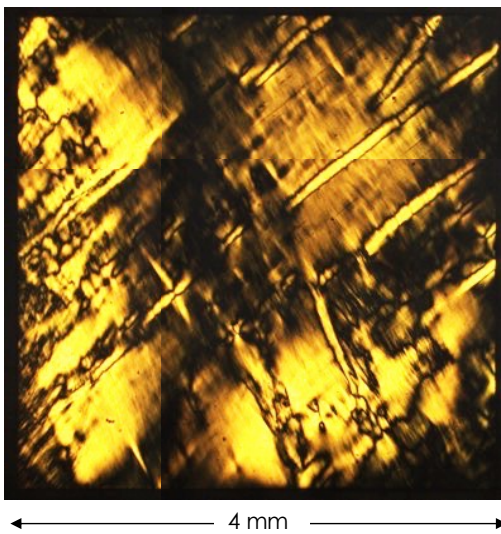
- Comparison SLM vs standard process.

	Std.	SLM
Resistivity	1 Ωcm	0.1 Ωcm
Diameter	~3μm	~1μm
Diamond to graphite ratio	~4	~0.2



28.05.24

X-polariser image

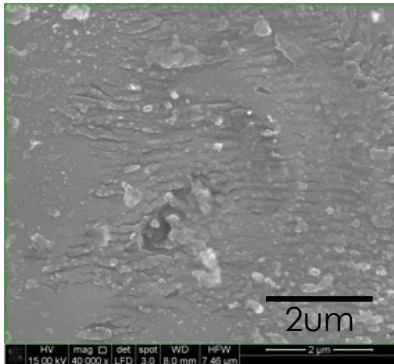
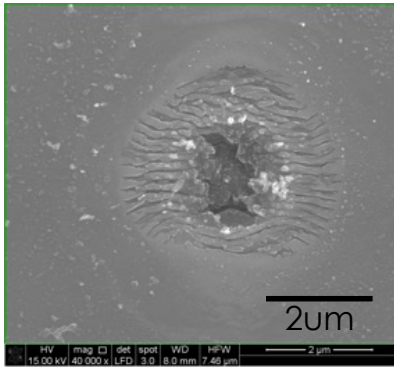


- Optical grade scCVD diamond.

- Post processing.

28.05.24

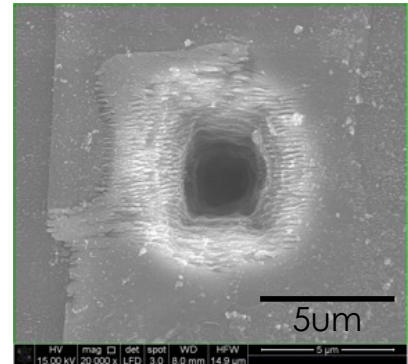
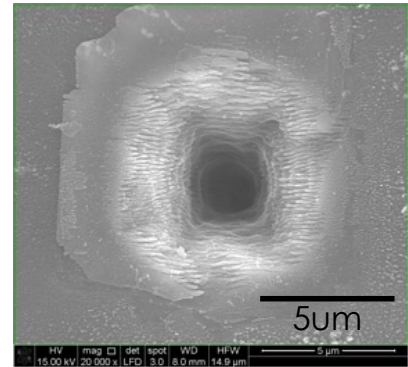
• Seed surface



With SLM
10µm/s
400nJ

Without SLM
10µm/s
400nJ

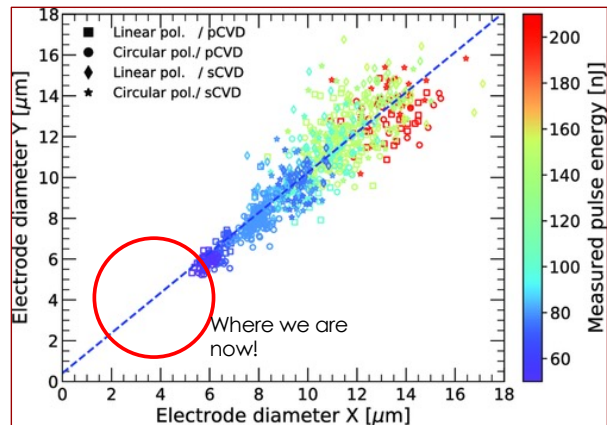
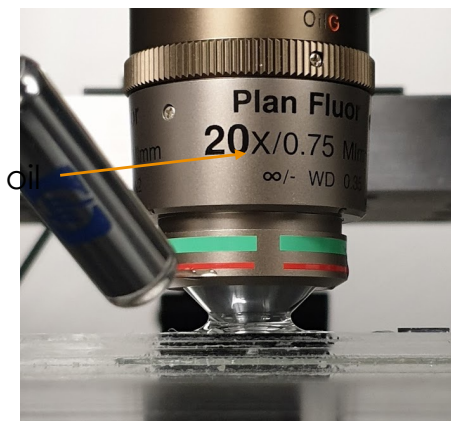
• Exit surface



28.05.24

Making the thinnest column

- More energy = thicker column
- Non-linear breakdown of diamond
 - More focused beam spot at depth makes thinner column
 - Immersion Oil helps to reduce refraction loss from air-diamond interface
 - SLM still key!

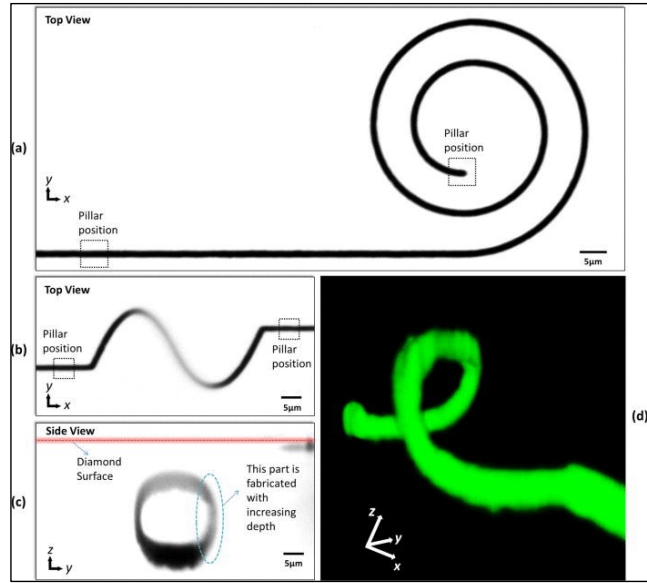


Lopez Paz, I., Allegre, O., Li, Z., Oh, A., Porter, A. and Whitehead, D. (2019), Study of Electrode Fabrication in Diamond with a Femto-Second Laser. Phys. Status Solidi A, 216: 1900236.

28.05.24

Moving sideways

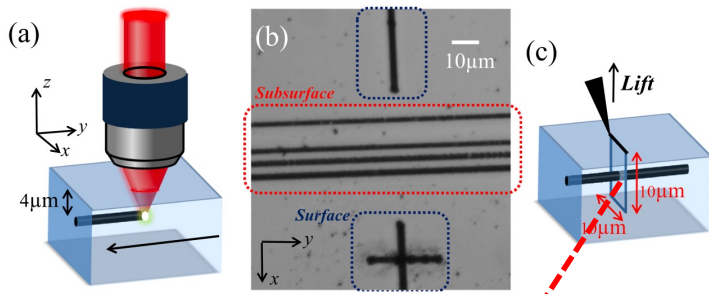
- Also have the possibility to move in **arbitrary** direction
- Wavefront correction needs to be tailored in real-time
 - For vertical columns have mainly spherical corrections
 - For horizontal processing, the correction is ~elliptical
- Gets even trickier at depth >200µm



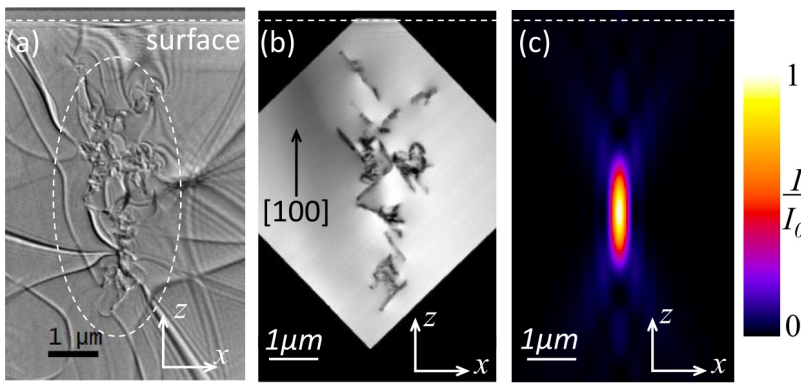
Sun, B., Salter, P. S., & Booth, M. J. (2014). High conductivity micro-wires in diamond following arbitrary paths. *Applied Physics Letters*, 105(23), 231105.

28.05.24

Internal structure



Patrick S. Salter et al., APPLIED PHYSICS LETTERS 111, 081103 (2017)



- Prepare sample with horizontal graphitic wires.
- STEM image of wire cross section.
- Optical and spectral data points to micro-cracks and nano-clusters of sp² bonded carbon.
- Micro wires are not macroscopic structures!

28.05.24

Parameter space scan

Patrick Salter, Oxford
Iain Haughton, AO, Manchester

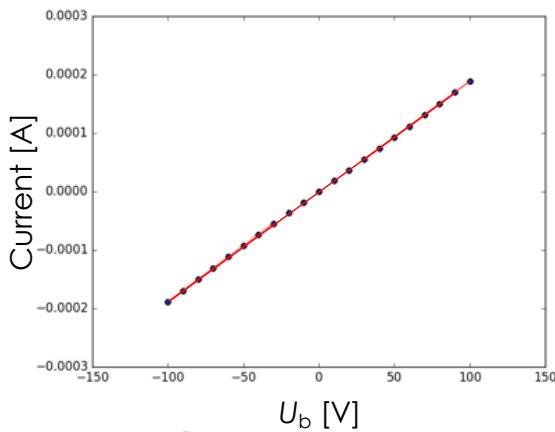
		Laser translation speed			
		5um/s	10um/s	20um/s	30um/s
Laser beam energy	100nJ	x	x		
	200nJ	x	x	x	
	300nJ		x	x	x
	400nJ		x	x	x
	500nJ			x	x
	600nJ				x

- Repeat **with** and **without** SLM correction.

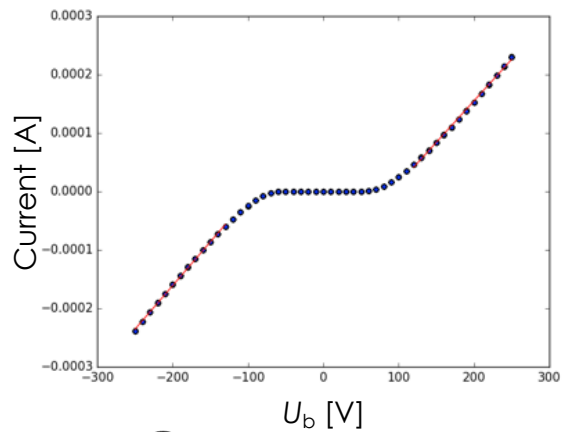
28.05.24

IV curves

- Ohmic and barrier potential curves observed.



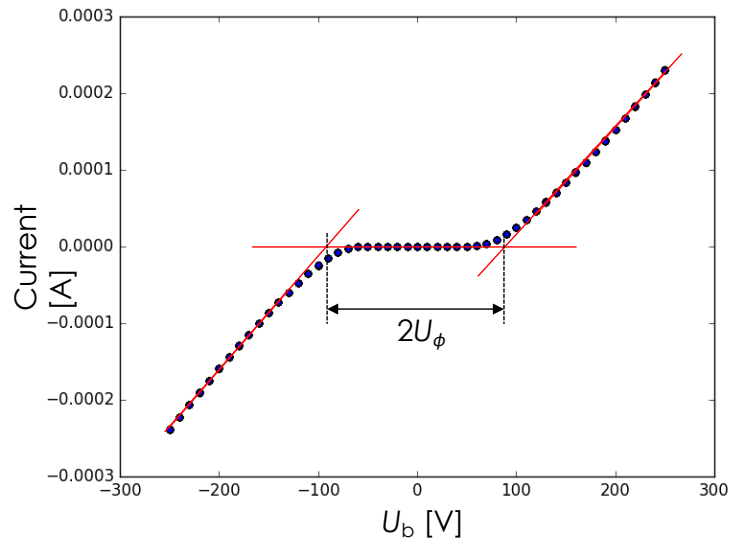
Continuous.



Bulk effect?
Micro gaps?

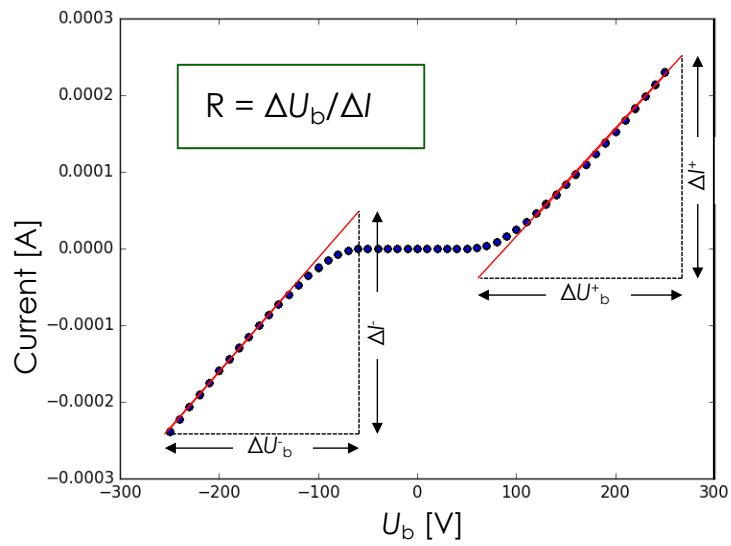
28.05.24

Barrier potential



28.05.24

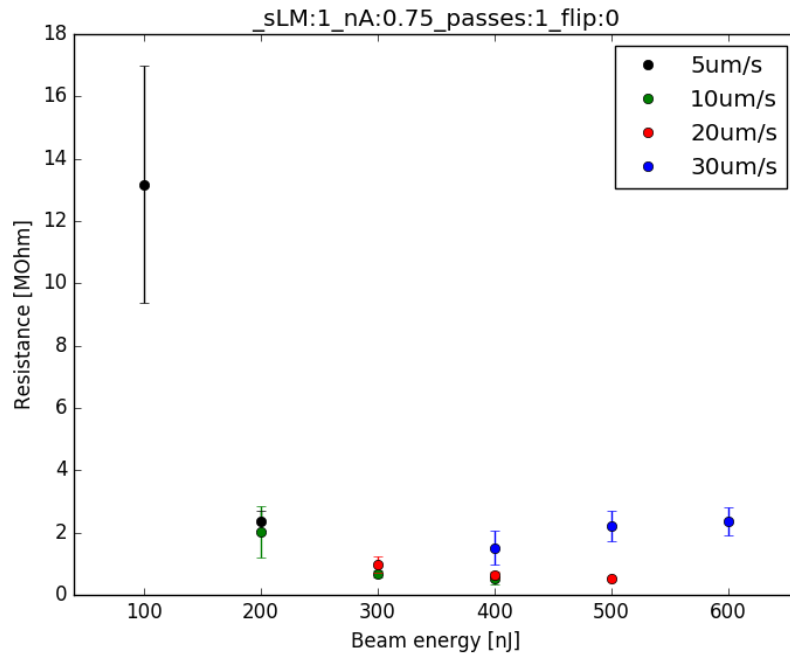
Resistance measurement



28.05.24

Resistance

81

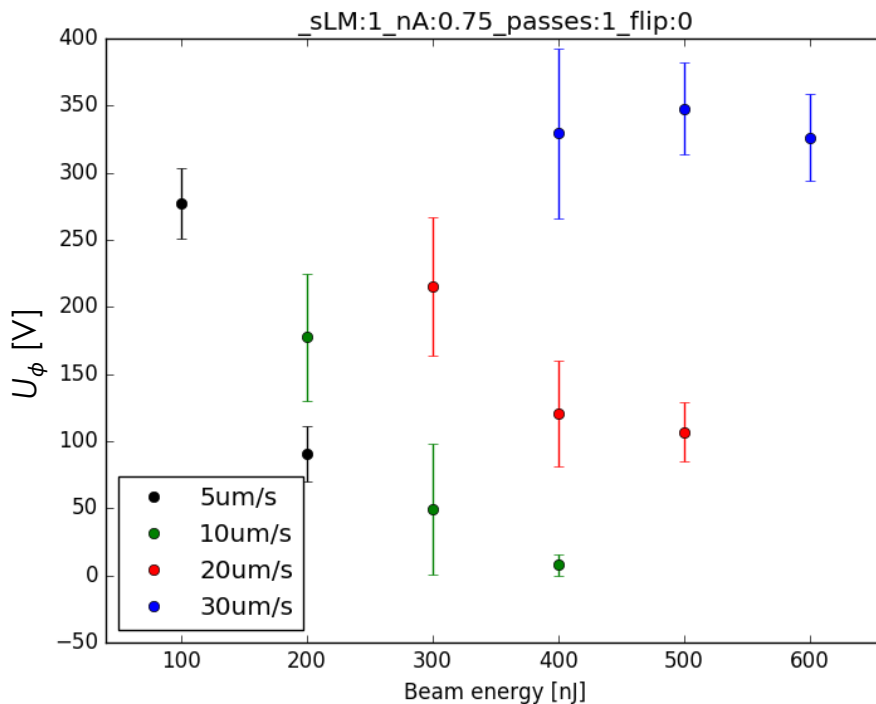


- Resistance increase as power law
→ multi-photon process.
- Clear discrepancy at 30 μm/s.

28.05.24

Barrier energy

82

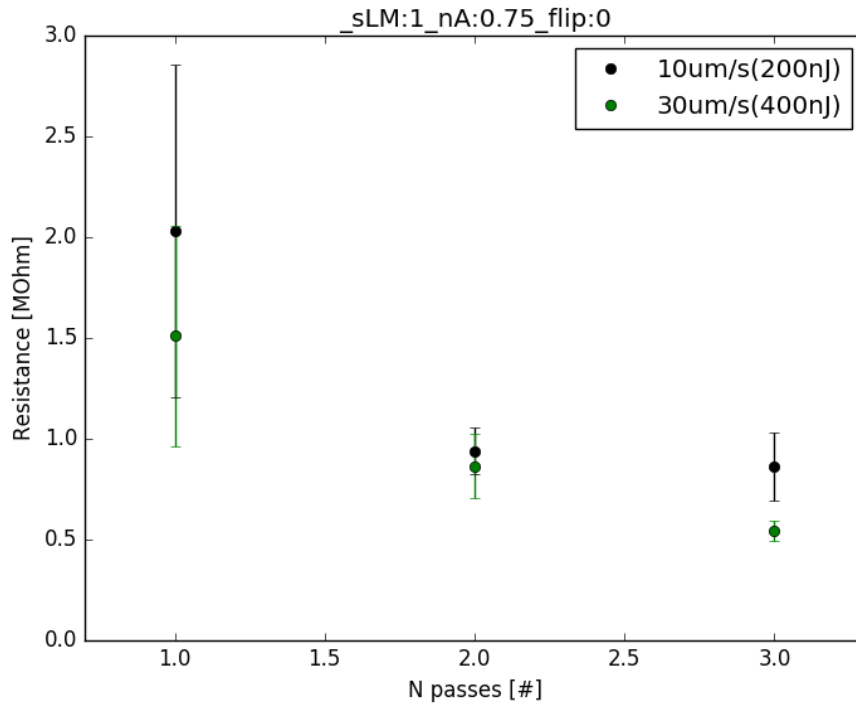


- Reduction in barrier with increased energy.
- Discrepancy at 30 μm/s.

28.05.24

Multiple passes

83

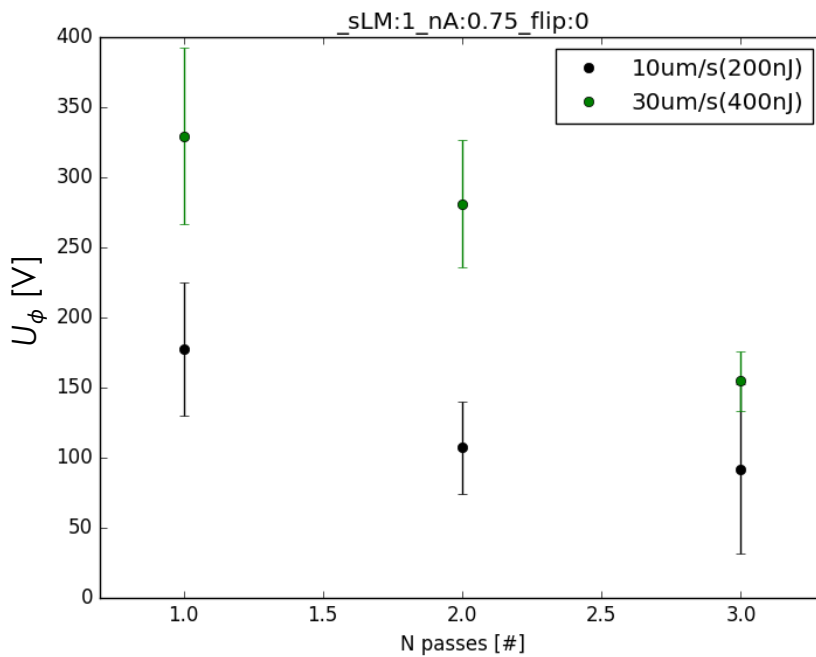


- Multiple passes reduces resistance and increases uniformity of the columns.

28.05.24

Multiple passes

84

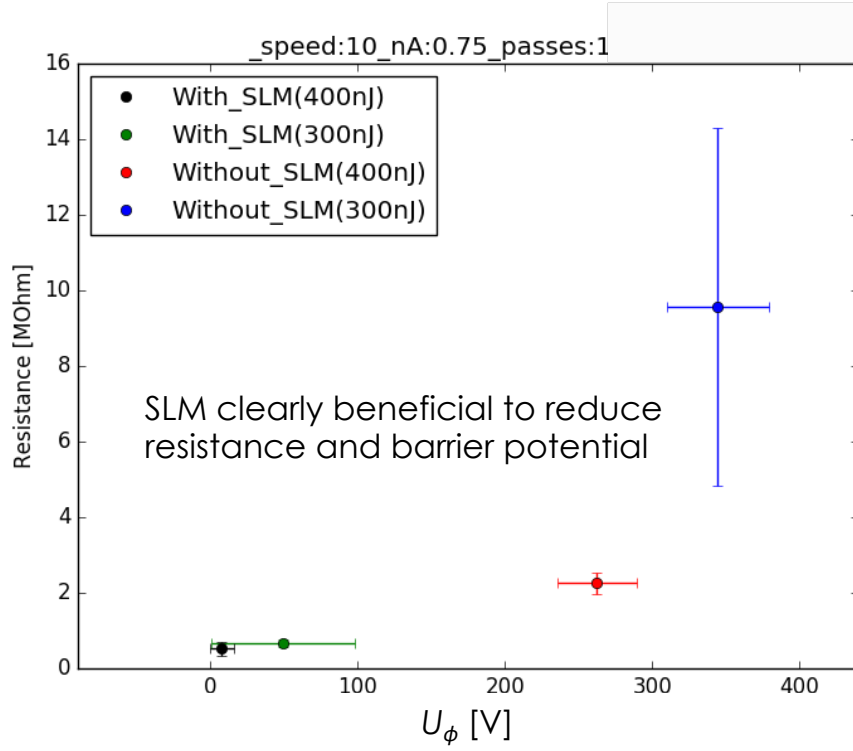


- Multiple passes also reduces U_ϕ .

28.05.24

With and without SLM

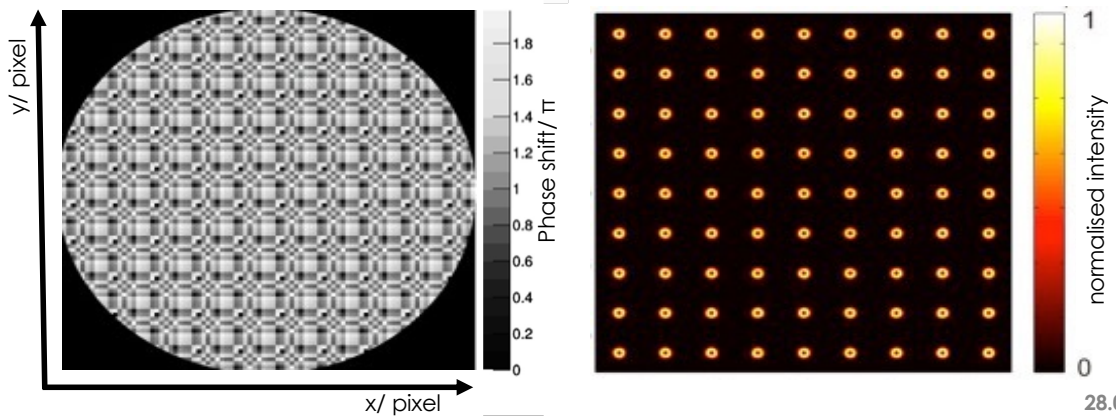
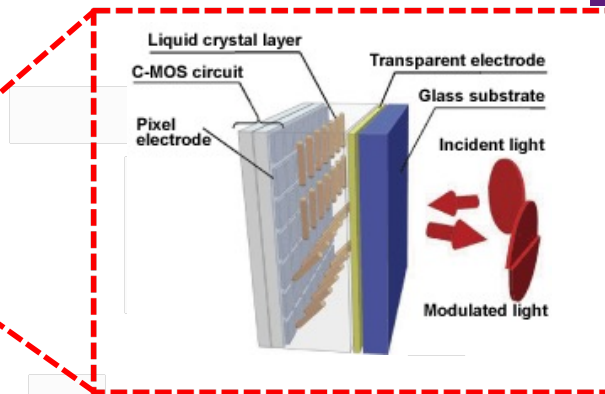
85



28.05.24

SLM parallel processing?

86



28.05.24

3D Diamond detector tests with relativistic charged particles

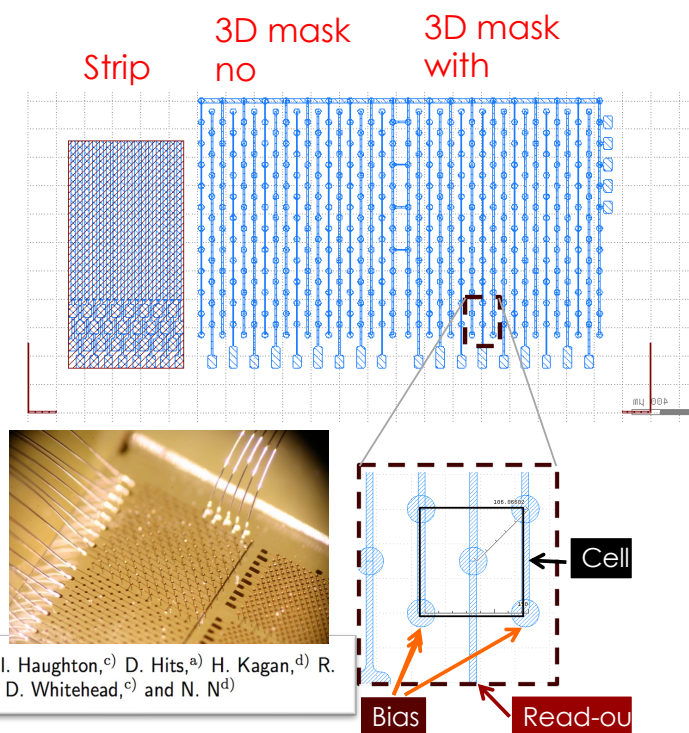
- Types
 - 100x100um cell size ganged to form strips
 - 100x100um cell size, bonded to pixel read-out
 - 50x50um cell size, bonded to pixel read-out
- All detectors made from polycrystalline diamond.
- Beam tests
 - CERN beam line H6 : protons ~ 120 GeV/c
 - PSI : pions ~ 250 MeV/c

Thanks for material from the RD42 collaboration!

28.05.24

3D Diamond prototype

- **Proto-type**
 - Strip detector with back side contact
 - 3D metal only pattern
 - 3D metal + graphitic columns
 - Cubic cell base size 150µm
 - 99 cells
- Measure response with 120 GeV protons.
- Paper published NIMA "A 3D diamond detector for particle tracking", NIM A, 786 (2015)



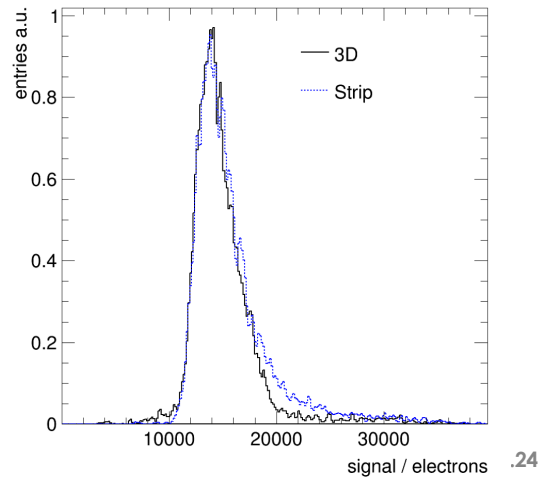
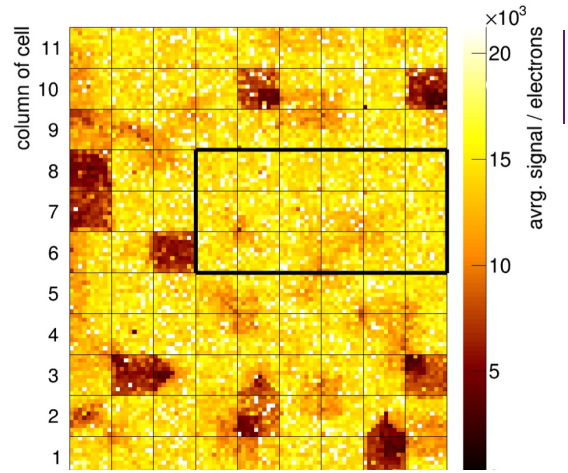
F. Bachmair,^{a)} L. Baeni,^{a)} P. Bergonzo,^{b)} B. Caylar,^{b)} G. Forcolin,^{c)} I. Haughton,^{c)} D. Hits,^{a)} H. Kagan,^{d)} R. Kass,^{d)} L. Li,^{e)} A. Oh,^{c)} M. Pomorski,^{b)} V. Tyzhnevyy,^{c)} R. Wallny,^{a)} D. Whitehead,^{c)} and N. N^{d)}

28.05.24

Analysis steps

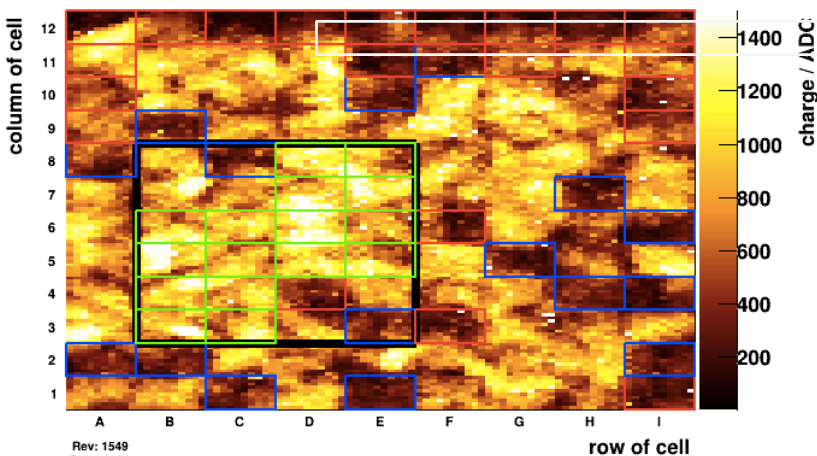
- $U_b(3D)=40V$
- $U_b(strip)=500V$
- Identify **continuous region** of intact cells for analysis.
- Exclude contribution of negative signals.
- **Average charge**
Strip: 16.8ke
3D: 15.9ke
- **MP:**
Strip: 14.7ke
3D: 15ke

3D and Strip show comparable response.
Conclusion -> 3D works!



Test of first 3D **pCVD** diamond detectors

hPulseHeightVsDetectorHitPostionXY_trans

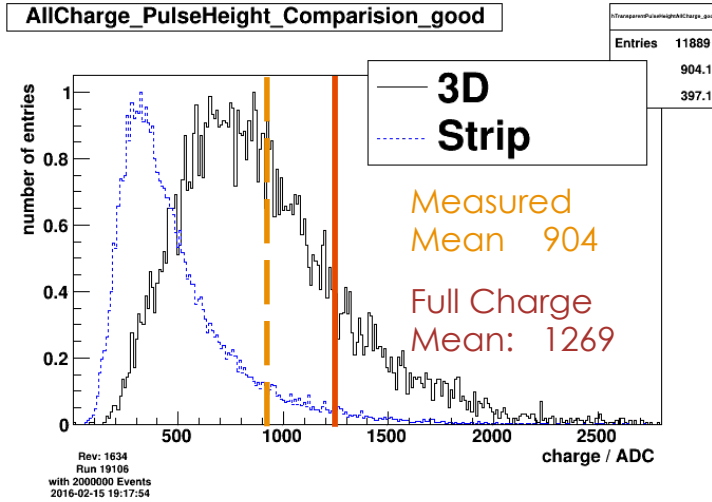


Rev: 1549
Run 19106
with 2000000 Events
2016-02-02 13:34:21

- $U_b(3D)=75V$
- $U_b(strip)=500V$
- Selected 16 adjacent cells

Test of first 3D **pCVD** diamond detectors

- Red line estimate the Mean for Full Charge Collection (100%)



71% of Full Charge Collection, corresponding to ~13 ke.

Highest charge collection ever measured for pCVD diamonds

28.05.24

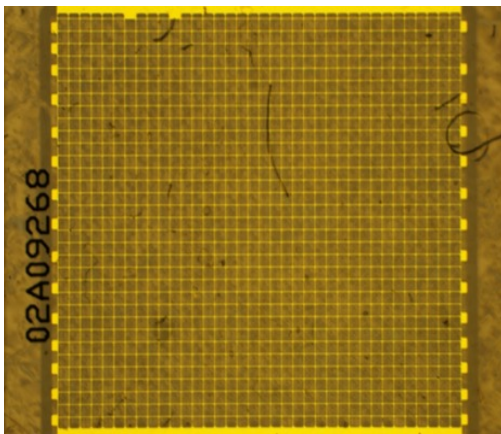
Large area 3D, pCVD, 100x100

92

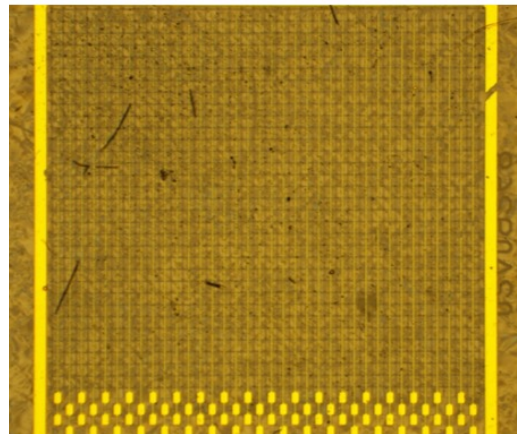
In May/Sept 2016 tested the first full 3D device fabricated in pcCVD with three dramatic improvements:

1. An order of magnitude more cells (1188 vs 99).
2. Smaller cell size (100um vs 150um).
3. Higher column production efficiency (>99% vs ~90%).

HV side



Readout side

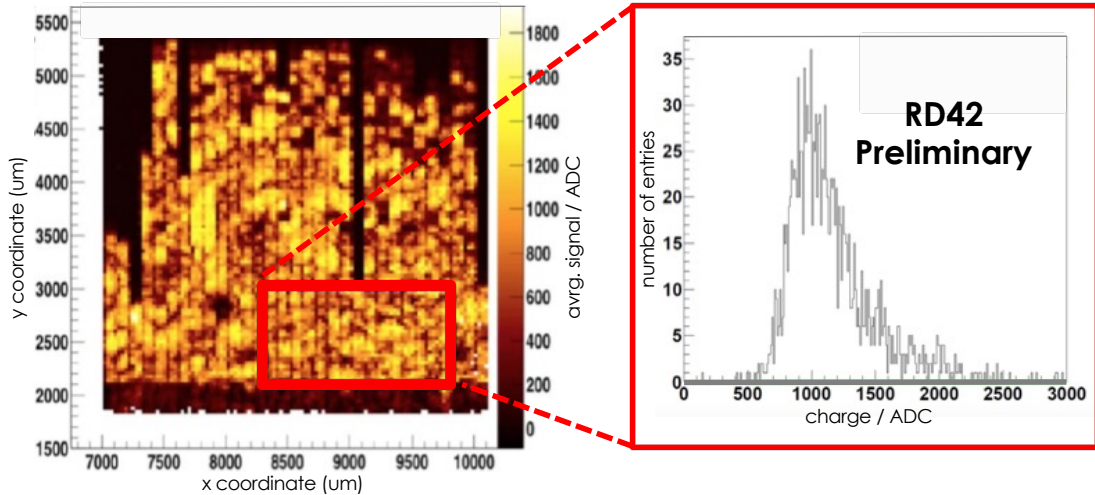


28.05.24

Large area 3D, pCVD, 100x100

93

- Largest charge collection to date in pcCVD diamond!
 - >85 % of charge collected in continuous region, about twice as much as planar.

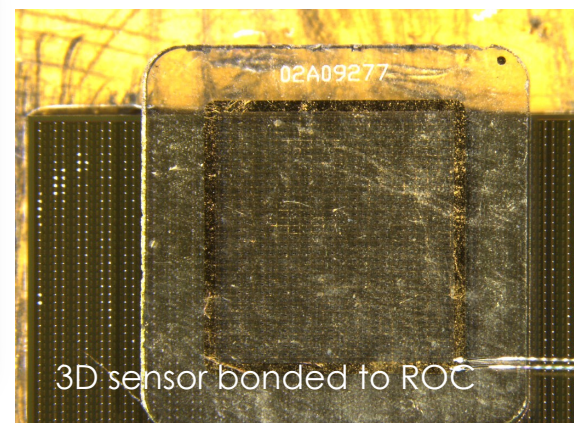
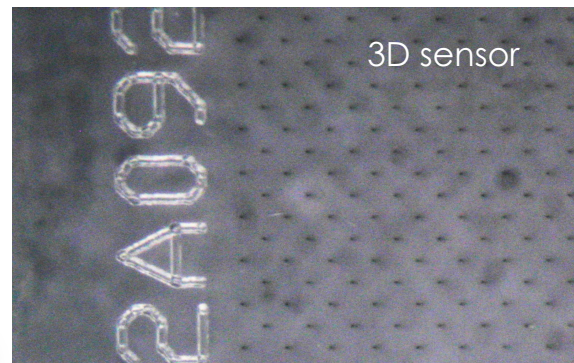
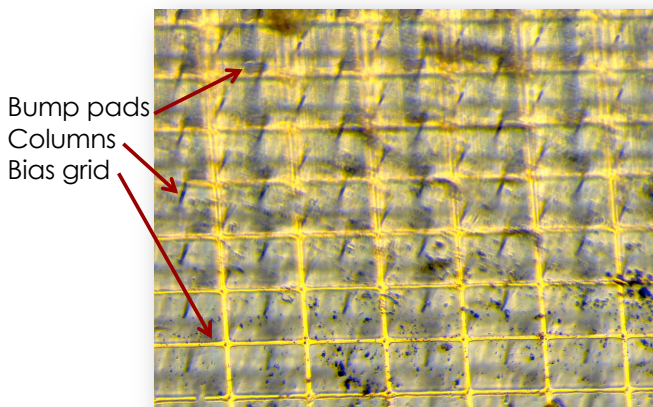


28.05.24

Pixel 3D, pCVD, 100x100

94

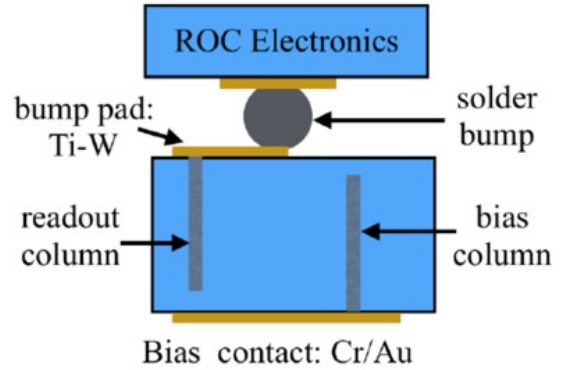
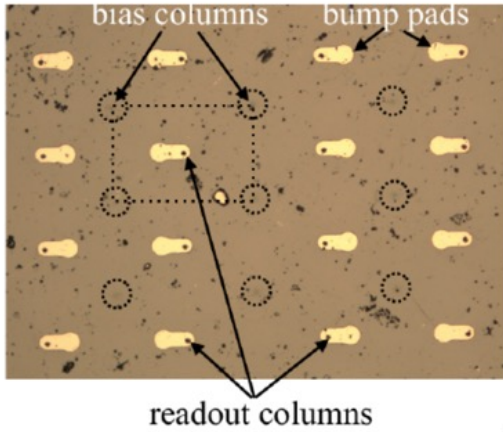
- First assembly with ROC chip produced.
 - Bump bonded in Princeton.
 - Cr-Au on bias side.
 - Ti-W under-bump metal.
 - Indium bumps on sensor.



24

Pixel 3D, pCVD, 100x100

- Production of first pixel device using CMS readout electronics.

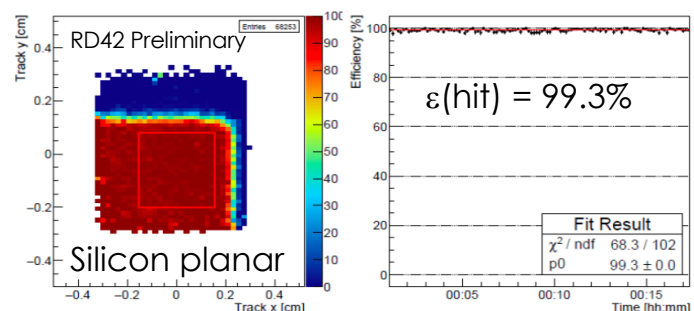
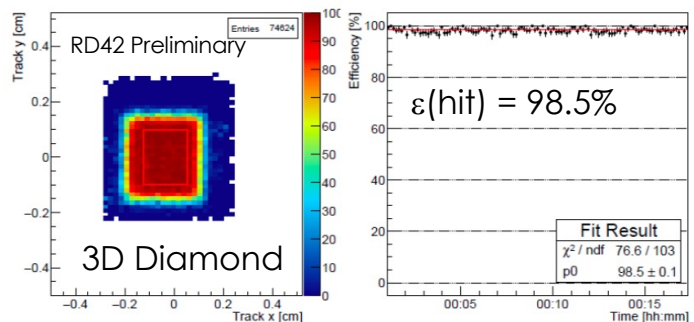


- Active region 3x3 mm with cell size ~100x100 um.

28.05.24

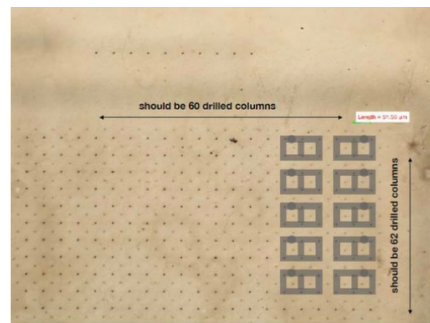
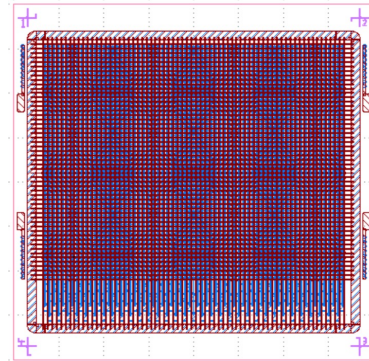
Pixel 3D, pCVD, 100x100

- 3D diamond device and Silicon reference planar device.
- Pixel threshold 1500e.
- Check hit efficiency over time.
- Device works!



Next generation 3D Diamond

- Produced 3500 Cell pixel prototype, 50x50um cell size.
- Sample production:
 - Oxford (2x cubic cells)
 - Manchester set-up in progress (expected production date end of month.)
 - Bump bonding
 - For ROC (CMS) Princeton.
 - For FE-I4 (ATLAS) IFAE.
- Data taking in August 2017 at PSI.

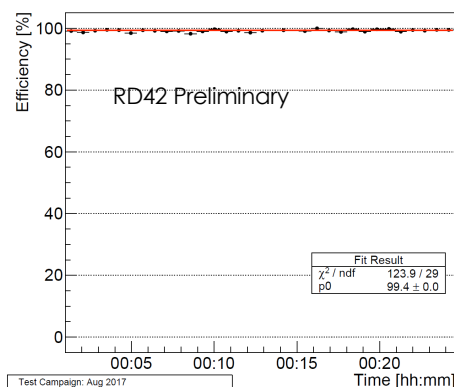
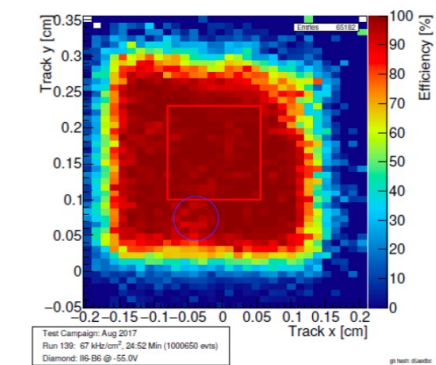


28.05.24

First 50x50 μm cell 3D Diamond (2017)

- Readout with CMS pixel readout.
- Bump bonding issue in upper right edge (Indium bump deposition machine not working properly)
- 6 columns (3x2) ganged together.
- Preliminary hit efficiency **99.2%**
- Preliminary: Collect **>90%** of charge!
- Rate dependence tested with 10 kHz/cm² and 10 MHz/cm² -> no dependence observed.

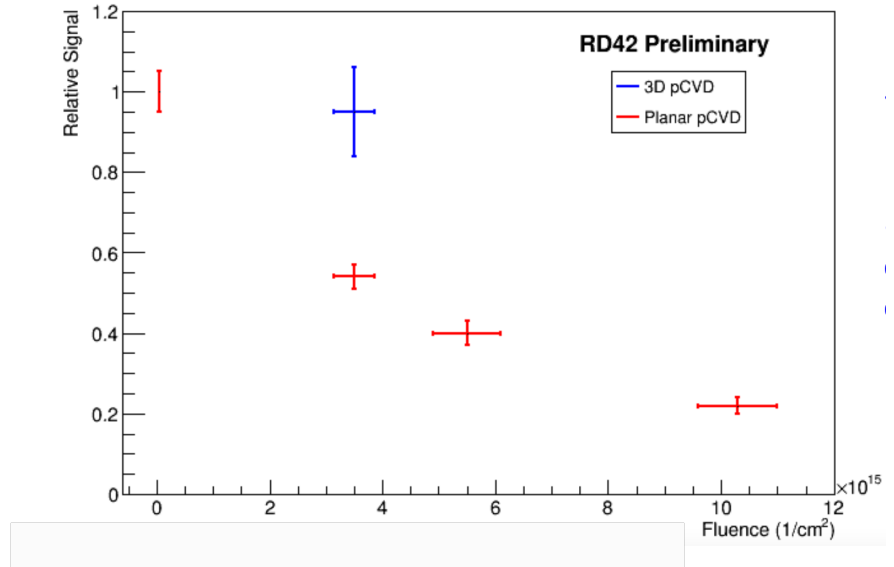
RD42 Preliminary



24

3D diamond radiation tolerance

- Tested a 3D device irradiated to 3.5×10^{15} p/cm² and compare to a planar diamond device at same fluence.
- Signal reduction:
Planar $45 \pm 5\%$
3D $5 \pm 10\%$
- Assuming scaling is similar 3D should operate at 10×10^{17} p/cm²



28.05.24

Applications in HEP

28.05.24

Applications in HEP

- Vertex detectors with CVD Diamond are not considered yet as an option for LHC.

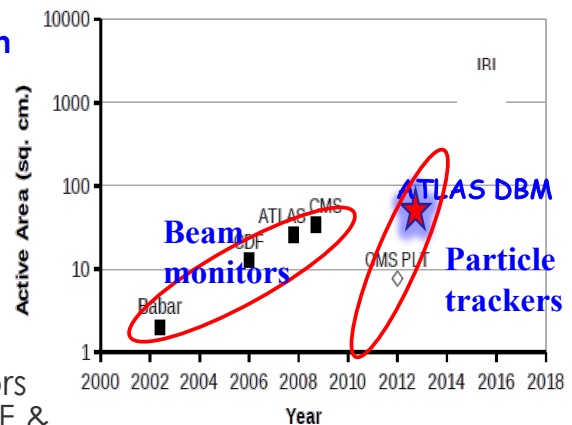
- For Beam monitoring CVD Diamond is used at CMS and ATLAS at the LHC.

- BaBar and Belle test already CVD Diamond in their beam monitoring system.

28.05.24

Diamond in current HEP experiments

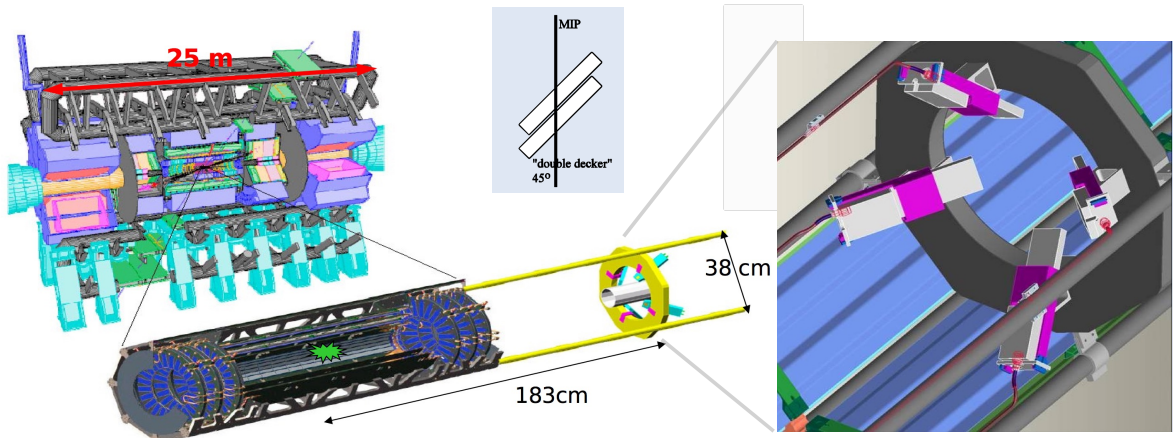
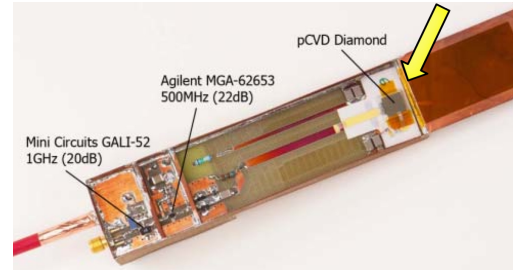
- **Beam monitors** to protect experiments against **beam losses** at the LHC, CERN.
 - For Silicon Vertex systems careful monitoring is crucial.
 - Beam monitors have to be **radiation hard**.
 - Abort beam when monitors signal dangerous beam conditions.
 - False signals must be avoided.
- During run-1 **diamond beam monitors operated** in ATLAS, CMS, and LHCb.
- Previously diamond beam monitors were installed in BaBar(SLAC), CDF & D0 (Tevatron).



28.05.24

ATLAS beam conditions monitor

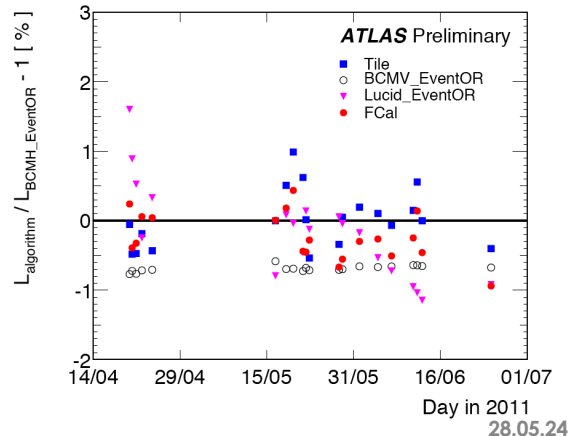
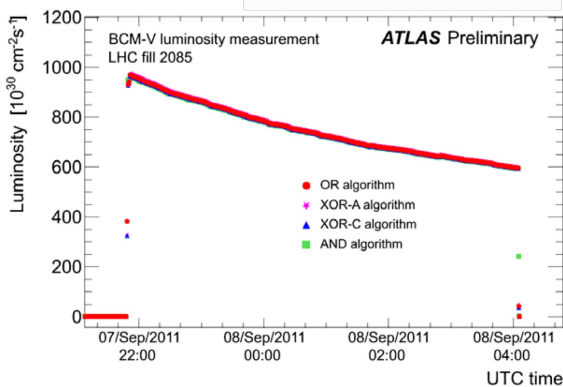
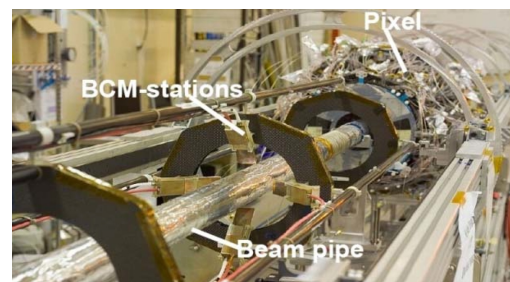
- Use 2x polycrystalline CVD diamonds per station (10 x 10 mm).
- 4 stations on each side of the ATLAS pixel detector
 - $z = \pm 183.8$ cm (~ 12.5 ns) and $r \sim 5$ cm



28.05.24

ATLAS beam conditions monitor

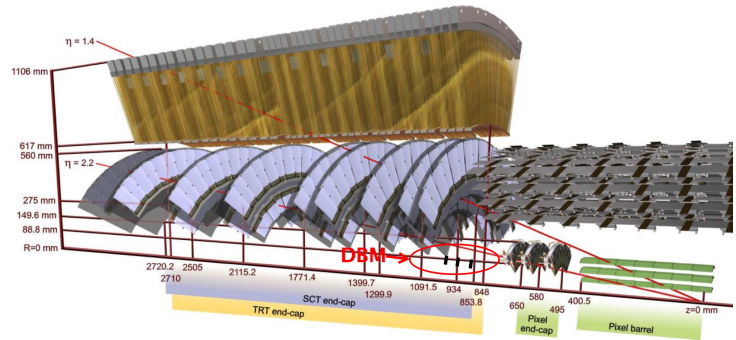
- Single particle counting with $\sigma=0.7$ ns.
- Distinguish between collision events and out-of-time background.
- Good stability
 - Used for luminosity determination.



28.05.24

Run 2: ATLAS Diamond Beam Monitor

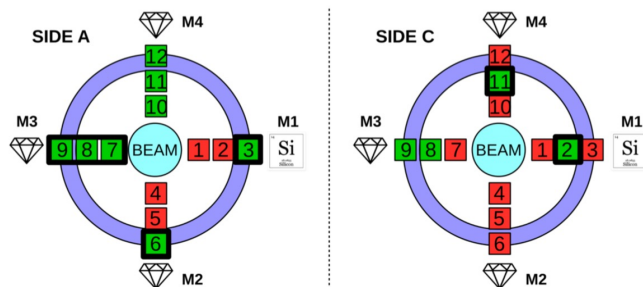
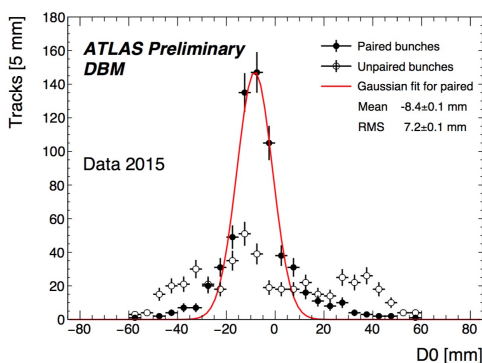
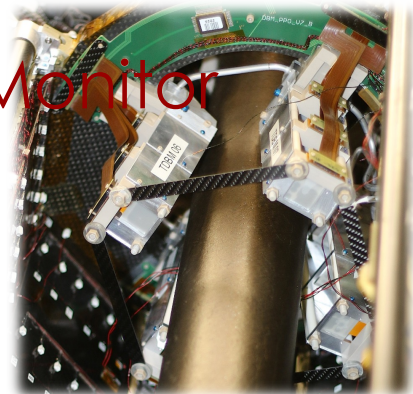
- 8 mini-trackers of 3 planes each using pixel-detectors.
- polycrystalline diamond sensors, 18mm x 21mm, $\delta > 250\mu\text{m}$.
- bump-bonded to FE-I4 pixel read-out chip.
 - 336 x 80 pixels
 - pixel size : $50\mu\text{m} \times 250\mu\text{m}$
- Purpose:
 - Bunch-by-bunch luminosity monitor (aim < 1 % per BC per LB)
 - Bunch-by-bunch beam spot monitor



28.05.24

Run 2: ATLAS Diamond Beam Monitor

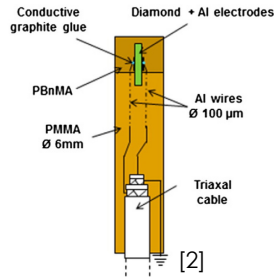
- Installed in ATLAS during LS1, but switched off due to unexpected death of Si and Diamond modules.
- DBM recommissioned in 2017/18 with 50% working modules.



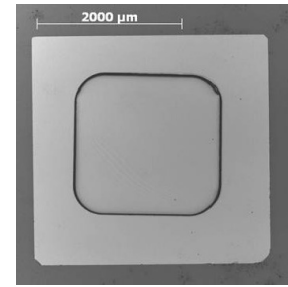
28.05.24

Examples of diamond detectors in related areas

- Synchrotron labs
 - beam position monitor
- Radiation Therapy
 - small field dosimetry
- Heavy Ion (GSI, FAIR)
 - beam diagnostic
 - particle tracking and TOF
 - hadron spectroscopy



scCVD dosimeter, 0,4 mm³ active vol. [2]



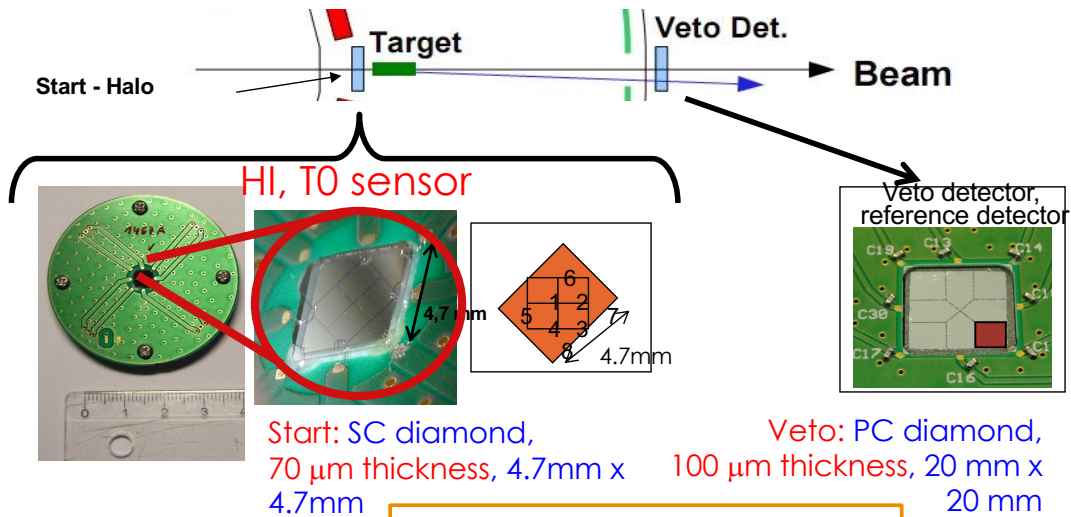
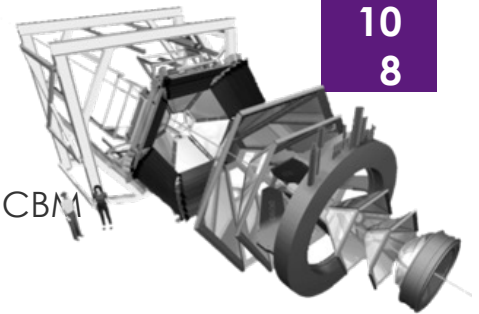
3 μm thick membrane in 40 μm thick scCVD [1]

[1] M. Pomroski, CEA-LIST, MRS Fall meeting, Boston 28/11/2012

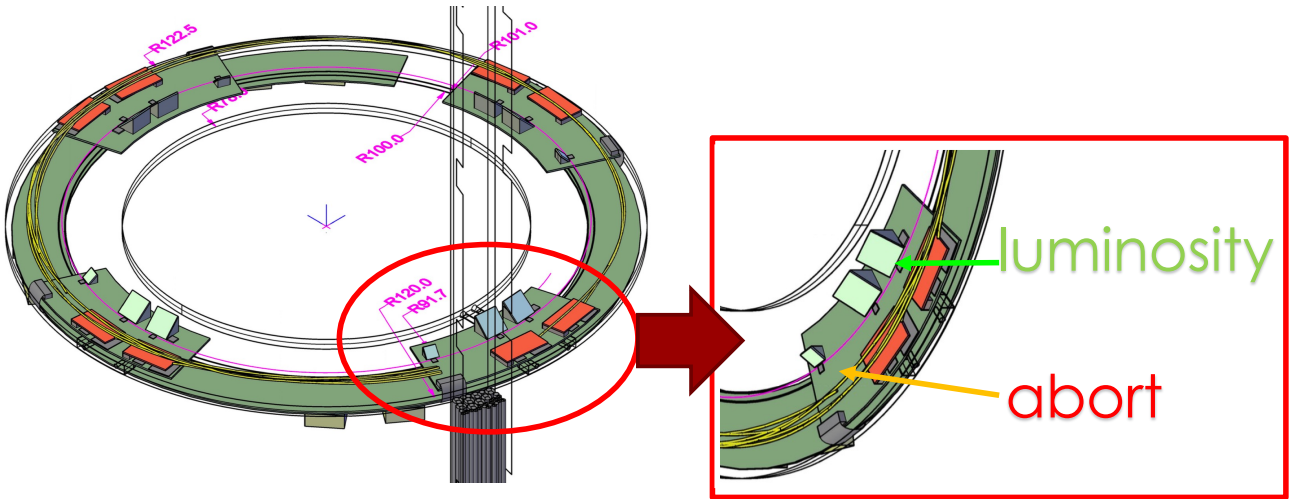
[2] F. Marsolat et al. / Diamond & Related Materials 33 (2013) 63-70.05.24

Detectors for Heavy Ion

- In-beam START-VETO detectors for HADES and CBM
 - High beam intensities (10⁷ #/s).
 - Protons (MIPS) up to very heavy ions (Au, U)
 - Excellent time resolution (30-100 ps)
 - Radiation hard up to 10¹² /cm Au ions



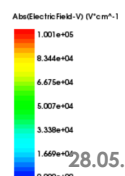
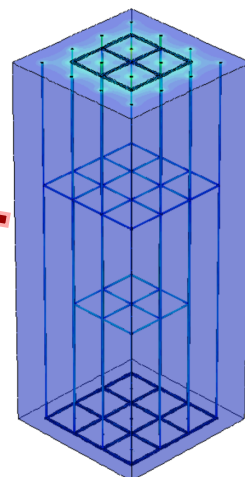
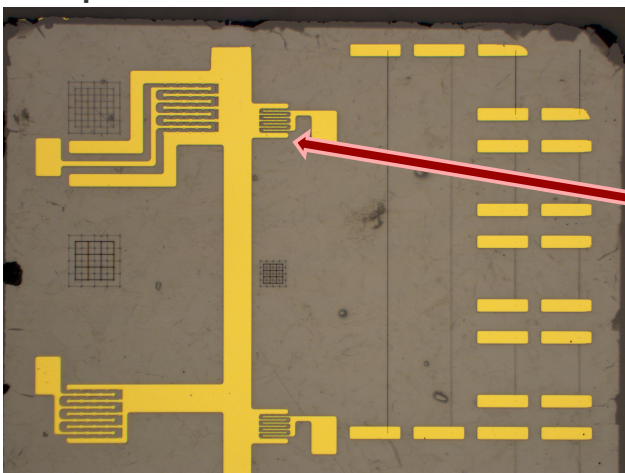
Upgrade for LHC Phase-2: BCM' modules



28.05.24

First BCM' 3D test structure with new "cage" design

- Fabricated March 2020 (~week of UK Lockdown) first 3D diamond device with horizontal ganging
- Test structure has horizontal wires at depths of 125 and 375 μm in a 500 μm thick substrate (ρ measurement)
- Metallised 3D detector with alternating ganging (~model) read out in current mode in **RD42 Zagreb Testbeam 06-2021, second version tested April 2022**



28.05.24

Dark matter

- Dark matter detection via elastic spin-independent interaction with Carbon nuclei.
- Diamond operated as cryogenic calorimeter.
- Reach of first prototypes is comparable to CRESST silicon sensors.
- Promising if scaled up (mass, time, background shielding)

Light dark matter search using a diamond cryogenic detector

CRESST Collaboration

G. Angloher¹, S. Banik^{2,3}, G. Benato⁴, A. Bento^{1,9}, A. Bertolini^{1,10}, R. Breier², C. Bucci¹, J. Burkhardt², L. Canonica^{1,13,16}, A. D'Addabbo¹, S. Di Lorenzo¹, L. Einfall^{2,3}, A. Erb^{6,10}, F. v. Feilitzsch⁴, S. Fichtinger², D. Fuchs¹, A. Garai¹, V. M. Ghete², P. Gorla¹, P. V. Guillaumont¹, S. Gupta¹, D. Hauff¹, M. Jeřkovič⁵, J. Jochum⁷, M. Kaznatcheeva¹, A. Kinast⁶, H. Kluck¹, H. Kraus³, S. Kuckuk¹, A. Langenkämper¹, M. Mancuso¹, L. Marini^{4,11}, B. Mauri¹, L. Meyer², V. Mokha¹, M. Ohmi¹, T. Ortmann⁶, C. Pagliarone^{4,12}, L. Pattavina^{4,6}, F. Petricca¹, W. Potzel⁶, P. Povinec², F. Pröbst¹, F. Pucci¹, F. Reindl^{2,3}, J. Roth⁶, K. Schäffner¹, J. Schieck^{2,3}, S. Schinner⁴, C. Schwertner^{2,3}, M. Stahlberg¹, L. Stodolsky¹, C. Strandhagen¹, R. Strauss¹, I. Usherov¹, F. Wagner², M. Willers⁴, V. Zema¹

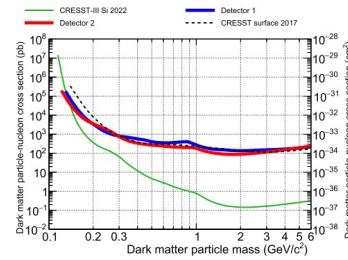


Fig. 5 Exclusion limits for the elastic spin-independent DM-nucleon scattering cross section at 90% CL, calculated for detector 1 (blue) and 2 (red) using Yellin's optimum interval method. In black, the previous best above ground exclusion limits of CRESST are plotted [17]. In green, the best exclusion limits below 0.160 GeV/c² from CRESST underground measurements [4] are plotted as a benchmark reference

28.05.24

Physics motivation

- Sensitive to dark matter and ALPs.
- Predictions for 1 kg Y *

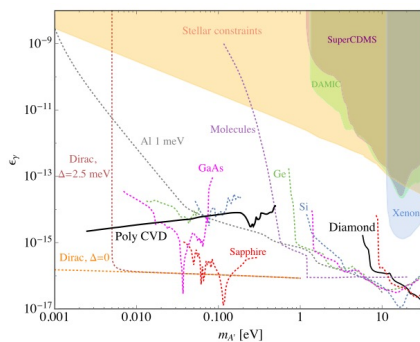


FIG. 4. Projected reach at 95% C.L. for absorption of kinetically mixed dark photons with mass greater than 1 meV. The solid black curves indicate the expected reach for a kilogram-year exposure of diamond. Projected reach for germanium and silicon [45], Dirac materials [10], polar crystals [12], molecules [82], and superconducting aluminum [9] targets are indicated by the dotted curves. Constraints from stellar emission [83,84], DAMIC [85], SuperCDMS [72], and Xenon [84] data are shown by the shaded orange, green, purple, and blue regions, respectively.

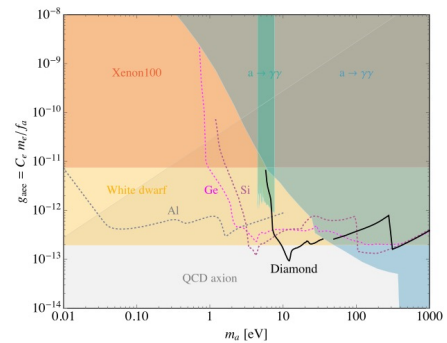


FIG. 5. Projected reach at 95% C.L. for absorption of axionlike particles. The reach of a kilogram-year exposure of diamond is shown by the solid black curve. The reach for semiconductors such as germanium and silicon [45] and superconducting aluminum [9] targets is depicted by the dotted magenta, purple, and gray curves, respectively. Stellar constraints from Xenon100 data [88] and white dwarves [87] are indicated by the shaded red and orange regions, respectively. Constraints from loop-induced couplings to photons are presented in the shaded blue and green regions [89,90]. The QCD axion region of interest is indicated in shaded gray.

* 1kg high purity synthetic diamond costs O(1 M)

28.05.24

Current Diamond TES landscape

- Relatively new field.
- Diamond proposed as a DM detector in 2019.

PHYSICAL REVIEW D 99, 123005 (2019)

Editors' Suggestion

Diamond detectors for direct detection of sub-GeV dark matter

Noah Kurinsky,^{1,2} To Chin Yu,^{3,4} Yonit Hochberg,⁵ and Blas Cabrera³

¹Fermi National Accelerator Laboratory, Batavia, Illinois 60510, USA

²Kavli Institute for Cosmological Physics, University of Chicago, Chicago, Illinois 60637, USA

³Department of Physics, Stanford University, Stanford, California 94305, USA

⁴SLAC National Accelerator Laboratory, 2575 Sand Hill Road, Menlo Park, California 94025, USA

⁵Racah Institute of Physics, Hebrew University of Jerusalem, Jerusalem 91904, Israel

(Received 5 February 2019; published 10 June 2019)

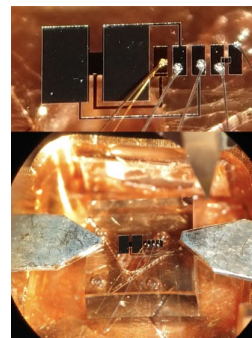
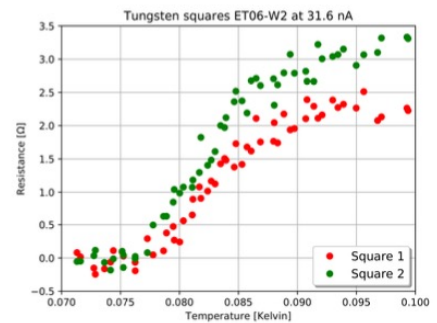
We propose using high-purity lab-grown diamond crystal for the detection of sub-giga electron volt dark matter. Diamond targets can be sensitive to both nuclear and electron recoils from dark matter scattering in the mega-electron-volt and above mass range as well as to absorption processes of dark matter with masses between sub-electron volts to tens of electron volts. Compared to other proposed semiconducting targets such as germanium and silicon, diamond detectors can probe lower dark matter masses via nuclear recoils due to the lightness of the carbon nucleus. The expected reach for electron recoils is comparable to that of germanium and silicon, with the advantage that dark counts are expected to be under better control. Via absorption processes, unconstrained QCD axion parameter space can be successfully probed in diamond for masses of order 10 eV, further demonstrating the power of our approach.

DOI: 10.1103/PhysRevD.99.123005

28.05.24

Why diamond?

- Operation as Transition Edge Sensor (TES)
 - W Al metalisation
- Diamond has high Debye temperature:
 - high thermal conductivity
 - excellent phonons transport.
- Light nucleus ($A=12$)
 - probe lower DM masses



Material	Θ_D in K
Diamant	1860
Si	645
Cr	610
Fe	470
Mo	450
Al	428
Ge	374
Cu	345

28.05.24

Summary

- Diamond systems are used as beam and luminosity monitors in current HEP experiments and foreseen for future experiments.
- Radiation hardness and rate dependence has been studied.
- 3D diamond has been demonstrated to work.
- The understanding of diamond as a detector material is advancing.